

## ELECTROPHORETIC DEPOSITION AS AN EFFECTIVE AND SIMPLE PROCESSING TECHNIQUE FOR FABRICATION OF MAGNESIUM SILICATE HYDRATE (M-S-H) COATINGS ONTO STAINLESS STEEL SUBSTRATES †

UDC 549.691.2 : 691.714.018.8

**Marjan Randelović, Jelena Čović, Aleksandra Zarubica, Aleksandar Bojić**

Department of Chemistry, Faculty of Sciences and Mathematics, University of Niš, 33 Višegradska St., 18000 Niš, Serbia

**Abstract.** *Magnesium silicate hydrate (M-S-H) was prepared via one-pot hydrothermal synthesis and electrophoretically deposited (EPD) onto stainless steel substrate (Type 304), varying different process parameters. The optimal conditions for the EPD process were found to be as follows. A stable suspension of material was achieved using isopropanol containing 1% water as dispersing medium and Mg-nitrate as charging additive. The best coating was obtained after three successively repeated EPD processes at a voltage of 30 V, accompanied by drying at room temperature between each EPD cycle. The coating showed a thickness of 31 μm and very smooth surface. After calcination at 900 °C coating retains its adherence to the substrate but undergoes a structural transformation from poorly crystallized M-S-H to well-crystallized clinoenstatite phase which is known for its biocompatibility. As a result, it densifies and shrinks giving grainy and slightly rough surface. Structural properties and parameters of the magnesium silicate hydrate (M-S-H) and clinoenstatite were acquired by XRD technique, while morphology was examined by the analysis of SEM micrographs. This study demonstrates that: i) M-S-H can be synthesized through simple hydrothermal route starting from simple, low-cost precursors, ii) EPD process is an effective technique for deposition of M-S-H materials onto stainless steel and iii) inosilicate mineral (clinoenstatite) can be successfully obtained from M-S-H by calcination at 900 °C.*

**Key words:** *electrophoretic deposition, clinoenstatite, magnesium silicate hydrate, hydrothermal*

---

Received September 9<sup>th</sup>, 2018; accepted January 20<sup>th</sup>, 2019

**Corresponding author:** Marjan Randelović

Department of Chemistry, Faculty of Sciences and Mathematics, 33 Višegradska St., 18000 Niš, Serbia

E-mail: hemija@gmail.com

†Acknowledgment: This work was supported by the Serbian Ministry of Education, Science, and Technological Development through the framework of the project TR 34008.

## 1. INTRODUCTION

Electrophoretic deposition (EPD) is a traditional processing method in the ceramic industry that is gaining increasing interest for production of new materials coatings. EPD is achieved through the movement of charged particles dispersed in a suitable liquid towards an electrode under an applied electric field (Bobruk et al., 2018; Boccaccini et al., 2010; Besra et al., 2007). This movement results in the accumulation of the particles and in the formation of a homogeneous deposit at the appropriate electrode. The main requirement to obtain an efficient EPD process is to use suitable suspensions where ceramic particles are well dispersed. Metals, polymers, ceramics, glasses and their composites can be deposited by EPD. Due to the numerous advantages of EPD, its application alone or in combination with other techniques has led to the development of advanced material (nano)structures including a variety of functional, nanostructured and composite coatings, layered and functionally graded materials, thin films, porous biomaterials, tissue scaffolds, drug delivery systems and biosensors, and also for the deposition of biopolymers, bioactive nanoparticles, carbon nanotubes (CNTs) and biological entities (e.g. proteins) in advanced nanostructured biomaterials and devices (Bobruk et al., 2018; Boccaccini et al., 2010; Besra et al., 2007; Farrokhi-Rad et al., 2018 a; Farrokhi-Rad et al., 2018 b; Mohammadi et al., 2018; Shehayeb et al., 2017; Sorrell et al., 2011; Rojaee et al., 2014).

Magnesium silicate hydrate (M-S-H) is a semi-amorphous phase which has been widely examined as potential low-pH-cements (Nied et al., 2016; Lothenbach et al., 2015). In the literature M-S-Hs have been considered as poorly crystalline Mg-silicates with a 2:1 magnesium phyllosilicate-like (talc-like) structure (Nied et al., 2016; Brew et al., 2005; Roosz et al., 2015). It was first discovered in 1953. during an investigation on the deterioration mechanism of concrete in seawater (Tran et al., 2017). The formation of the magnesium silicate hydrate (M-S-H) was described as a detrimental phenomenon associated with sulfate attack on concrete (Lothenbach et al., 2015; Bernard et al., 2017). Besides its natural occurrence, M-S-H phases have also been synthesized in the laboratory. However, under laboratory conditions, M-S-H formation is very slow with equilibration period of about 1 year (Nied et al., 2016). Moreover, there are no studies which concern nor a hydrothermal synthesis of M-S-H neither its chemical transformation to pyroxene group of inosilicates, such as clinoenstatite which is known as bioceramics.

Bioceramics have been widely used for the replacement or regeneration of the musculoskeletal system and in dental applications (Goudouri et al., 2014; Chu et al., 2008; Curtis and Watson et al., 2008; Mala et al., 2018; Diba et al., 2014). According to their chemical surface reactivity, bioceramics can be classified in bioinert, bioactive and bioresorbable materials (Diba et al., 2014). Bioactive materials are of special interest in this study due to their ability to form chemical bonds with living tissues. In the context of orthopedic implants, the bioactivity of a material usually (but not necessary) implies the formation of an apatite layer on its surface upon immersion in biological fluids. Previous relevant studies have shown that the composition of bioceramics is one of the key parameters affecting their biocompatibility, bioactivity, and biodegradability (Hench et al., 2002). Moreover, the release of specific elements (ions) from bioactive materials can induce positive effects in their surrounding biological environment. Magnesium is very important mineral elements in the human body, with approximately half of the total

physiological magnesium stored in bony tissues. Several studies have indicated that divalent cations (e.g.  $Mg^{2+}$ ) have a key role in bone remodeling and skeletal development (Diba et al., 2014; Wu et al., 2015).

In addition to the traditional hydroxyapatite coating material, magnesium-containing inorganic materials are in the focus of numerous biomaterials research gaining even more important over time (Diba et al., 2014; Wu et al., 2015). Various Mg-containing silicate ceramics have been shown to be bioactive and attractive for biomedical applications (Diba et al., 2014). These materials have been proven to promote cell adhesion, proliferation, spreading, and differentiation, which make them promising candidates for tissue engineering applications (Wu et al., 2015). As can be seen, due to its fundamental role in cellular processes and human metabolism, Mg possesses high relevance for biomedical applications. On the other hand, silicon (Si) is an essential trace element for bone development. These studies suggest that Mg and Si have osteoimmune modulatory effects that favor osteogenesis (Diba et al., 2014).

Clinoenstatite ( $MgSiO_3$ ) contains both Mg and Si combining mechanical strength with chemical stability and cytocompatibility (Wu et al., 2015). For these reasons, it is considered an ideal coating material for orthopedic metal implants.

In spite of their qualities, metals and alloy implants frequently trigger a foreign body reaction in which the implant is encapsulated in a fibrous layer between implant and bone (Wu et al., 2015). Therefore, the immune response usually leads to the failure of metal-based implants to integrate with the skeleton and it is necessary to apply coating materials with beneficial osteoimmunomodulatory properties which enhances the integration between coating materials and surrounding host bone tissue and favors bone regeneration. Another important requirement is to achieve high bonding strength in the interface between the coating material and metal substratum which could support a greater functional load while the coating material integrates with the new bone tissue.

The current paper reports the hydrothermal synthesis and characterization of M-S-H gel as well as its structural transformation to clinoenstatite at a calcination temperature of 900 °C. Additionally, optimal parameters for electrophoretic deposition of M-S-H onto stainless steel substrate have been presented and discussed. Immobilization of M-S-H onto metallic substrates in the form of thin coatings and subsequent calcination could be important for its application in biocompatibility improvement of metals.

## 2. MATERIALS AND METHODS

### 2.1. Magnesium silicate hydrate (M-S-H) synthesis

For the purpose of magnesium silicate hydrate (M-S-H) synthesis, analysis-grade reagents  $Mg(NO_3)_2 \cdot 6H_2O$  and  $Na_2SiO_3 \cdot 5H_2O$  (Sigma-Aldrich) were used. In the synthesis, 1:1 mol ratio of reagents had been weighted and each was dissolved in 35 ml of deionized water. Then, these two solutions were mixed by adding Na-metasilicate solution to Mg-nitrate solution and stirred for 30 min on a magnetic stirrer. Then, produced milky slurry was transferred into a Teflon-lined stainless steel 316 L autoclave. The closed reactor was heated in a furnace for 8 h at 200 °C at the autogenous pressure, without stirring. At the end of treatment, the autoclave was spontaneously cooled to room temperature. The precipitate formed was filtered on Buchner funnel under vacuum and

washed with plenty of deionized water. Finally, the samples were dried in air at 120 °C for 3 h, crushed in an agate mortar and passed through 150 mesh sieve. The obtained solid phase was used for electrophoretic deposition onto conductive stainless-steel substrate.

## 2.2. Electrophoretic deposition

The electrophoretic deposition (EPD) experiments were carried out at a temperature of 25 °C, in a two-electrode system. The working electrode as a substrate for deposition of the Mg-silicate nanoparticles and the counter electrode were placed in a Pyrex cell. Working electrodes were composed of 304 type stainless steel (S.S.), the dimensions of 78x25x0.4 mm, while the counter electrode was chosen to be Ti sheet. Prior to any experiment the working electrodes were mechanically polished and sonicated in deionized water and ethanol. After that, they were electrochemically polished in 0.5 M solution of oxalic acid with a constant current of 0.5 A.

Iso-propanol containing 1 % water was selected as the dispersion medium, and magnesium nitrate was used as the charging additive for the nanoparticles. The charging additive was first added to the solution, and then mixed for approximately 15 min to obtain a homogeneous charging medium. Subsequently, Mg-silicate powder was slowly added to the solution containing the charging additive, and the suspension was then ultrasonicated for 30 min to create a uniformly dispersed system.

The two electrodes were immersed in the prepared EPD suspension and connected to a DC power supply (BK Instruments programmable DC power supply). The working and counter electrodes were then used as the cathode and anode, respectively. Electrophoretic deposition was performed at a constant voltage of i) 10 V; ii) 20 V and iii) 30 V for 3 min. The corresponding current was 0.01 A, while the working distance between the cathode and anode was 7 mm. EDP at 30 V was successively performed three times with ultrasonication of suspension for 3 min between EPD cycles in order to obtain a final coated substrate which was dried at room temperature. The mass of deposited Mg-silicate coatings with the surface of 40x25 mm was determined by weighing the cathode before and after deposition. Coated S.S. samples were then thermally treated for 2 h at a temperature of 900 °C in order to obtain clinoenstatite phase. The heating rate was 7.5 °C/min.

The microstructures of the Mg-silicate materials and coatings on S.S. substrates were investigated using a scanning electron microscopy (SEM) using a JEOL JSM-6610LV and digital microscope Motic D-EL1. Coatings and powders were analyzed by X-ray diffraction, using a Rigaku diffractometer model Ultima IV diffractometer running with CuK $\alpha$  radiation. In order to understand the strain associated with the sample caused by lattice deformation, line broadening analysis and calculations were carried out by using the Williamson-Hall (W-H) method based on the following equation:

$$\beta_{hkl} \cos \theta = \frac{K\lambda}{D} + 4\epsilon \sin \theta \quad (1)$$

where  $\beta$  is integral width,  $\theta$  is the Bragg angle,  $k$  is shape factor,  $\lambda$  is the wavelength of the X-rays used,  $D$  is crystalline size,  $\epsilon$  is the micro strain. The strain value was obtained from the graph by the use of the W-H method.

### 3. RESULTS AND DISCUSSION

#### 3.1. Characterization of fabricated M-S-H

##### 3.1.1 XRD

Powder X-ray diffraction (PXRD) analysis of Mg-silicate powder obtained by hydrothermal treatment revealed that there are no sharp diffraction peaks in the XRD pattern suggesting the presence of low crystalline phases (Fig. 1a). The broad diffuse peaks at 19.77, 26.14, 34.95 and 59.94 °2θ are in good agreement with the XRD data reported for M-S-H (Nied et al., 2016; Lothenbach et al., 2015; Brew et al., 2005; Roosz et al., 2015).

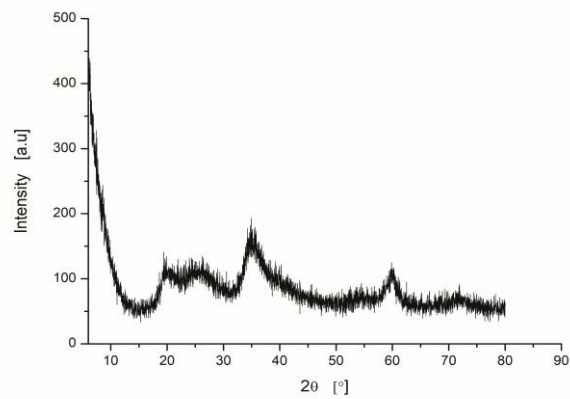


**Fig. 1a.** The X-ray diffraction pattern of M-S-H

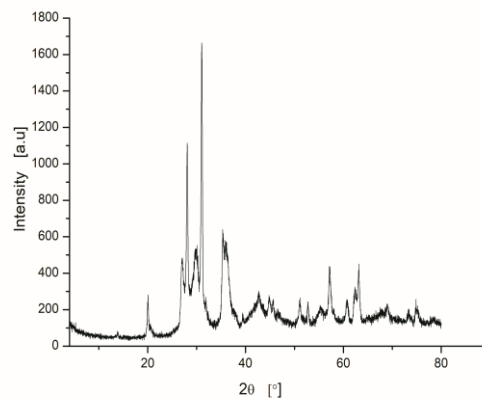


**Fig. 1b.** The X-ray diffraction pattern of clinoenstatite

Roosz et al. suggest that the M-S-H is composed of nano-crystalline and turbostratic Mg–Si phyllosilicates that cannot be straightforwardly be related to any known mineral (Roosz et al., 2015). Recent studies indicate that the peak positions correlate well to the

main peaks of talc at 19.5, 28.6, 36.1 and 60.5 °2θ and explain the broad, diffuse peaks by a defect talc structure of M-S-H (Nied et al., 2016). However, calcinations of M-S-H powder and surface coatings at 900 °C resulted in the dehydroxylation and collapse of the defect phyllosilicate sheets forming clinoenstatite as the dominant crystalline phase (Fig 1b).

All the diffraction peaks of the calcined sample with a full width at half maximum (FWHM) are listed in Table 1 and could be clearly indexed to clinoenstatite in accordance with the reported JCPDS data (card no. 19-769).

**Table 1** Peak list

No.	2-theta(deg)	Height(cps)	FWHM(deg)
1	13.92	101.9	0.90
2	19.99	197	0.44
3	26.94	342	0.90
4	28.02	841	0.34
5	29.90	383	3.13
6	30.99	1464	0.28
7	35.55	533	1.40
8	39.67	63.8	0.90
9	42.3	64	3.2
10	45.07	193.1	0.90
11	51.03	204.6	0.90
12	52.83	190.7	0.90
13	55.48	131.5	0.90
14	57.23	287	0.53
15	60.68	108	0.47
16	63.07	207	1.06
17	68.82	74	1.11

Based on the obtained results, the calculated crystallite size for clinoenstatite is 16.7 nm and micro strain is 0.68 %.

### 3.1.2. SEM

The morphology of nanoparticles has a crucial role in the mobility and preferred orientation of the nanoparticles in the electrolyte and may affect the uniformity and quality of the films. The SEM microphotographs of M-S-H in Fig. 2a illustrates that M-S-H exhibits particles of crushed gel with very sharp edges and diameter up to 10 μm. After calcination at 900 °C, particles acquire smooth round morphology due to a sintering process. Figure 2b shows the formation of necks at the contact points between adjacent round particles. Liquid phase formation at sintering temperature can be explained by the presence of small amount of Na<sup>+</sup> ions retained at the surface of M-S-H which act as a flux.

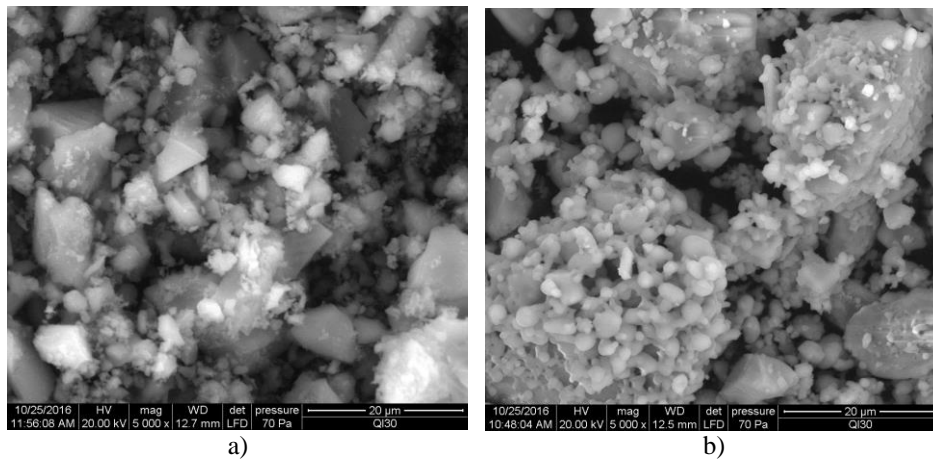


**Fig. 2.** SEM pictures of a) M-S-H and b) clionoenstatite

### 3.1.3. EPD

Optimal characteristics of suspension (conductivity, dielectric constant, particle size, zeta potential, etc) was achieved by using isopropanol with 1% of water as dispersing medium, finely ground Mg-silicate material and  $Mg^{2+}$  as charging additive.

Talbot et al reported that the magnesium nitrate dissociates providing positive ionic species due to the dissociation of  $Mg(NO_3)_2$  which increases the suspension conductivity, electrophoretic mobility, and the zeta potential of the suspended particles. As a result, upon the dissociation and hydrolysis of  $Mg(NO_3)_2$ , the  $Mg(NO_3)^+$  or  $MgOH^+$  ions surrounding the particles. The small amount of water present in the suspension induce minor electrolysis reactions after applying the electric field forming  $Mg(OH)_2$ , which acts as a binder material. Consequently, the stability of suspension and adherence of the material to the substrate are increased. Moreover, such composition ensures optimal electrical conductivity of suspension which is measured to be  $10.55 \pm 1.5 \mu S/cm$  and zeta potential +47 mV.

The change of the deposit weight of Mg-silicate per surface area as a function of the applied voltage during EPD is shown in Fig. 3.

The mass flow of particles toward the electrode with the opposite charge is proportional to the applied electrical field. As observed, the deposit weight increases as the voltage was increased.

The rate of migration that the particles can achieve is linearly dependent on the applied electric field (voltage). It is given by the Eq. 2:

$$v = \frac{zE}{6\pi\eta r} \quad (2)$$

where  $E$  is the applied electric field,  $\eta$  is the suspension viscosity,  $r$  is the particle radius and  $z$  is the particle charge.

When a particle reaches the cathode close enough, attractive forces dominate and coagulation/deposition occurs on S.S. substrate forming coating.

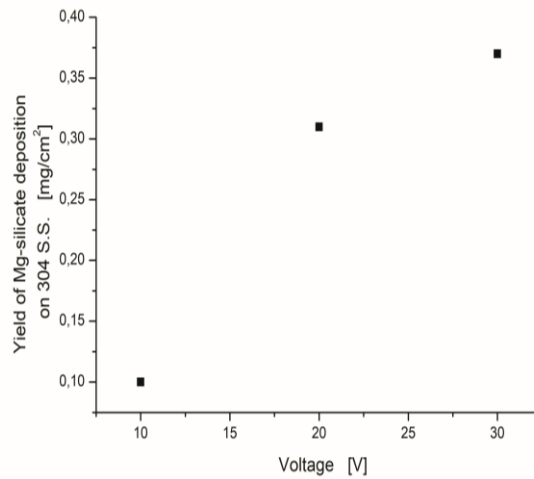


**Fig. 3.** The deposit weight per surface area vs. applied deposition voltage

According to Eq. (2), increasing the applied voltage increases the rate of particle migration and consequently increases the amount of deposit and coating thickness. At very low voltages, charged particles migrate very slowly and then agglomerate before reaching the electrode preventing their deposition. This might explain the low deposition thickness obtained at 10 V comparison with the other applied voltages.

In order to obtain the final coating onto a selected substrate, electrophoretic deposition was successively repeated three times at a voltage of 30 V. Multiple depositions were accompanied by drying at room temperature between each EPD cycle. The increasing of deposit weight per surface area of the substrate at each stage is shown in Fig.4.

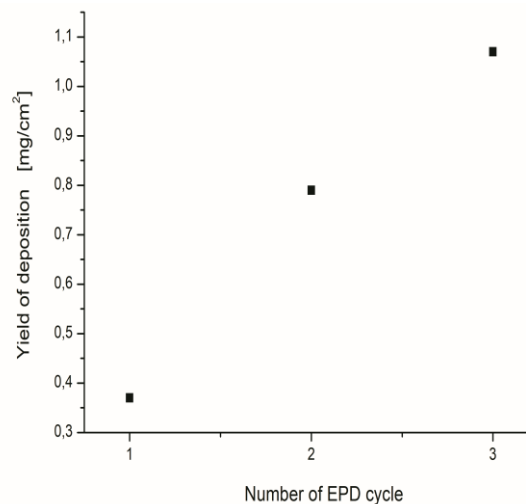


**Fig. 4.** The yield of deposition of M-S-H per surface area of SS substrate as a function during multiple deposition processes



However, at higher voltage thicker coatings increase the electrical resistivity of the working electrode, which decreases the current flow.

The change of the deposit weight of M-S-H per surface area of the substrate of stainless steel as a function of the distance between the electrodes during EPD is shown in Fig 5. As observed, the deposit weight of Mg-silicate decreases with an increase in distance between the electrodes.

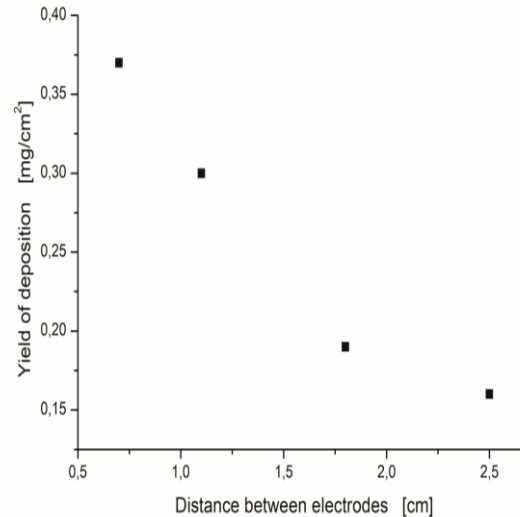


**Fig. 5** The deposit weight of Mg-silicate per surface area of the substrate of stainless steel as a function of the distance between the electrodes

When the distance between electrodes is greater, the effect of the electric field which occurs between them is weaker, the particles of the suspension material are moving slower and EPD is less efficient. The consequence of efficiency reduction is decreased in weight of the material.

The dependence of the weight of the deposited material on the stainless steel plate in the function of the deposition time is presented in Fig. 6. As shown, the deposit weight of Mg-silicate increases almost linearly as the duration of the process increases. The optimal straight line was obtained by standard regression analysis using the linear least squares fitting technique. The slope of the straight line is 0,00163 and gives the weight of the deposited material on the electrode per the unit of time and corresponds to the product  $\mu ESC$  in the Hamaker's equation.

$$m = \mu EtSC_s \quad (3)$$

where  $m$  is the mass of the deposit per unit area ( $\text{g}/\text{cm}^2$ ),  $\mu$  is the electrophoretic particle mobility ( $\text{cm}^2/\text{Vs}$ ) in the electric field  $E$  ( $\text{V}/\text{cm}$ ),  $t$  is deposition time,  $S$  is the surface of the electrode,  $C_s$  is the concentration of the solid phase in the suspension.

According to Sarkar et al., linear dependence indicates that the process took place under conditions of constant current and constant concentration of the suspension, which is confirmed by experimental observations during EPD [23]. During EPD, a constant current of 0,01 A is recorded at a constant voltage of 30 V. This is the simplest case of an

electrophoretic deposition which can be explained as a consequence of a migration–coagulation mechanism. This is valid only for a short deposition time, during which the deposit resistance has not significantly changed.

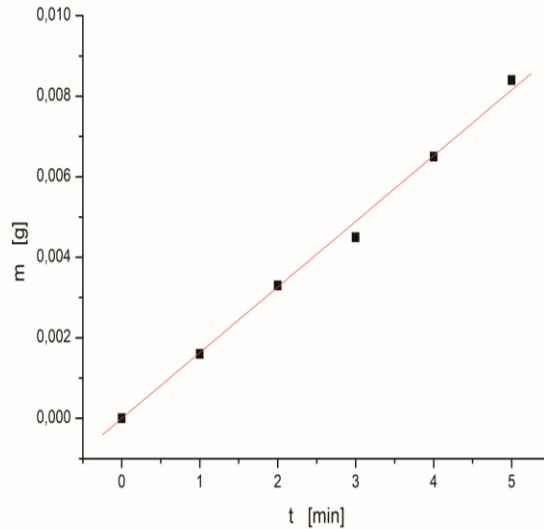


**Fig. 6** The deposit weight of Mg-silicate as a function of the deposition time

Comparative morphological characteristics of the substrate, electrochemically etched substrate, a final coating of Mg-silicate in its native form and after calcination at 900 °C were presented in Fig. 7.

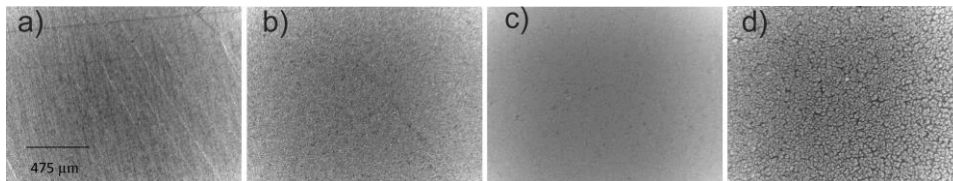


**Fig. 7** The micrograph of: a) S.S. substrate, b) electrochemically etched S.S. substrate, c) native Mg-silicate coating surface electrophoretically deposited on 304 S.S. substrate and d) Mg-silicate coating on the substrate after calcination at 900 °C.

S.S. substrate has a nonuniform and scraped surface which was polished by controlled corrosion of a metallic surface through electrochemical etching. Small scale roughness can be observed on the etched surface providing a good basis for EPD coatings.

After three repeated cycles of EPD, the very smooth and homogeneous surface of Mg-silicate coating with no visible cracks was obtained. According to the measurement performed with digital microscope Motic D-EL1, the Mg-silicate coating showed a thickness of 31 μm. After calcination (Fig. 7d) deposited layers show discrete grains of almost uniform size which is usually having in mind that during calcination and sintering, the coating undergoes a crystallization forming clinoenstatite phase. As a result, it densifies and shrinks, but the substrate typically does not change dimension significantly.

During this process, the coating will develop tensile stress in it and these stresses will be relieved by the formation of discrete grains which appear as small isolated islands.

#### 4. CONCLUSIONS

Amorphous M-S-H material was obtained by hydrothermal treatment in Si-Mg-Na-H<sub>2</sub>O system and electrophoretically deposited on stainless steel. In order to obtain high-quality coatings, isopropanol containing 1% water was selected as the dispersion medium, and magnesium nitrate was used as the charging additive for the nanoparticles. The observation by digital microscope showed a smooth, dense and homogeneous Mg-silicate coating on stainless steel. The best coatings were obtained by three successively repeated EPD processes at a voltage of 30 V, accompanied by drying at room temperature between each EPD cycle. The heat treatment of the coated samples at 900 °C induced the formation of clinoenstatite crystal phase which was proved for its bioactivity by many previous studies. Structural characteristics of coatings and powder materials were studied by XRD technique.

#### REFERENCES

- Bernard, E., Lothenbach, B., Rentsch, D., Pochard, I., Dauzères, A., 2017. *Phys. Chem. Earth*, 99, 142-157.
- Besra, L., Liu, M., 2007. *Prog. Mater. Sci.* 52, 1-61.
- Bobruk, M., Molin, S., Chen, M., Brylewski, T., Hendriksen, P.V., 2018. *Mater. Lett.* 213, 394-398.
- Boccaccini, A.R., Keim, S., Ma, R., Li, Y., Zhitomirsky, I., 2010. *J. R. Soc. Interface* 7, S581-S613. doi: 10.1098/rsif.2010.0156.focus
- Brew, D.R.M., Glasser, F.P., 2005. *Cement Concrete Res.* 35, 85-98.
- Chu, P.K., Liu, X., 2008. *Biomaterials Fabrication and Processing Handbook*, CRC press
- Curtis, V.R., Watson, F.T., 2008. *Dental biomaterials, Imaging, testing and modelling*, CRC press, Woodhead publishing limited
- Diba, M., Goudouri, O-M., Tapia, F., Boccaccini, R.A., 2014. *Curr. Opin. Solid St. M.* 18(3) 147-167.
- Farrokhi-Rad, M., 2018a. *J. Alloy. Compd.* 741, 211-222.
- Farrokhi-Rad, M., 2018b. *Ceram. Int.* 44, 622-630.
- Goudouri, O-M., Kontonasaki, E., Papadopoulou, L., Kantiranis, N., Lazaridis, N.K., Chrissafis, K., Chatzistavrou, X., Koidis, P., Paraskevopoulos, K.M., 2014. *Mater. Chem. Phys.* 145, 125-134.
- Hench, L.L., Polak, J. M., 2002. *Science* 295 (5557) 1014-1017.
- Lothenbach, B., Nied, D., Hôpital, E.L., Achiedo, G., Dauzères, A., 2015. *Cement Concrete Res.* 77, 60-68.
- Mala, R., Ruby Celsia, A.S., 2018. *Fundamental Biomaterials: Ceramics*, 195-221.
- Mohammadi, E., Aliofkhaeaei, M., Sabour Rouhaghdam, A., 2018. *Ceram. Int.* 44, 1471-1482.
- Nied, D., Enemark-Rasmussen, K., L'Hopital, E., Skibsted, J., Lothenbach, B., 2016. *Cement Concrete Res.* 79, 323-332.
- Rojaee, R., Fathi, M., Raeissi, K., Taherian, M., 2014. *Ceram. Int.* 40, 7879-7888.
- Roosz, C., Grangeon, S., Blanc, P., Montouillout, V., Lothenbach, B., Henocq, P., Giffaut, E., Vieillard, P., Gaboreau, S., 2015. *Cement Concrete Res.* 73, 228-237.
- Sarkar, P., Nicholson, S.P., 1996. *J. Am. Ceram. Soc.* 79(8), 1987-2002.
- Shehayeb, S., Deschanel, X., Karamé, I., Ghannam, L., Toquer, G., 2017. *Surf. Coat. Tech.* 322, 38-45.
- Sorrell, C.C., Taib, H., Palmer, T.C., Peng, F., Xia, Z., Wei, M., 2011. *Hydroxyapatite and Other Biomedical Coatings by Electrophoretic Deposition, Biological and Biomedical Coatings Handbook: Processing and Characterization*, Sam Zhang, 81-137.
- Tran, H.M., Scott, A., 2017. *Constr. Build. Mater.* 131, 526-535.
- Wu, C., Chen, Z., Wu, Q., Yi, D., Friis, T., Zheng, X., Chang, J., Jiang, X., Xiao, Y., 2015. *Biomaterials* 71, 35-47.

## **ELEKTROFORETSKA DEPOZICIJA KAO EFEKTIVNA I JEDNOSTAVNA PROCESNA TEHNIKA ZA DOBIJANJE MAGNEZIJUM-SILIKATNIH HIDRATA (M-S-H) NA SUPSTRATIMA OD NERĐAJUĆEG ČELIKA**

*Magnezijum-silikat-hidrat (M-S-H) je pripremljen hidrotermalnom sintezom, a zatim elektroforetski deponovan (EFD) na supstrat od nerđajućeg čelika (tip 304), pri čemu su menjani različiti parametri procesa elektroforetske depozicije. Utvrđeni su sledeći optimalni uslovi: u cilju dobijanja stabilne suspenzije materijala, kao disperzni medijum je korišćen izopropanol koji sadrži 1% vode, a kao aditiv za elektrostatičku stabilizaciju suspenzije nanočestica, korišćen je magnezijum-nitrat; prevlake najboljeg kvaliteta su dobijene nakon tri uzastopna EFD ciklusa pri naponu od 30 V, pri čemu se između svakog ciklusa elektroforetske depozicije prevlaka sušila na sobnoj temperaturi. Ovim postupkom je dobijena kompaktna prevlaka, ujednačene debljine, dobre adhezije i glatke morfologije. Nakon procesa kalcinacije na 900 °C na prevlaci se pojavljuju blage neravnine i zrnasta struktura, koja je posledica sinterovanja na primenjenoj temperaturi. Proces kalcinacije je rezultirao formiranjem kristalne faze klinoenstatita, što dokazuje da se nakon kalcinacije/dehidratacije magnezijum-silikat može vrlo lako transformisati u klinoenstatit, koji je poznat po svojoj biokompatibilnosti. Strukturne osobine M-S-H i klinoenstatita su ispitane XRD tehnikom, dok je morfologija ispitana SEM analizom. Ovo istraživanje je pokazalo da: I) M-S-H se može sintetisati hidrotermalnom sintezom; II) elektroforetska depozicija (EFD) je efikasna tehnika za deponovanje M-S-H materijala na nerđajućem čeliku; III) klinoenstatit se može uspešno dobiti kalcinacijom M-S-H na 900 °C.*

*Ključne reči: elektroforetsko deponovanje, klinoenstatit, hidratizani magnezijum-silikat, hidrotermalna sinteza*